Differential cross sections and spin density matrix elements for $\gamma p \rightarrow \phi p$ from the CLAS g11a dataset

Biplab Dey

Carnegie Mellon University

Hadron Spectroscopy Meeting, June 18^{th}, 2010

Outline

Outline

Introduction – $\phi(1020)$

- Belongs to the family of ground state vector mesons $V = \rho, \omega, \phi$.
- Almost pure $s\bar{s}$ state – OZI rule suppresses quark/meson exchanges during interaction with nucleons.
- Chief attraction – very "clean" system to study gluonic exchanges; gluonic structure of the Pomeron, for example.
- Near threshold and forward angles, access to the scalar glueball $J^P = 0^+$ expected (LQCD predicts mass ≈ 1.73 GeV).
- Around $\sqrt{s} = 2.2$ GeV, previous world data (LEPS, SAPHIR) saw a "bump" at $t \to |t|_{min}$. *Not* expected from Pomeron exchange – interference with $K^+\Lambda(1520)$?
- Very low cross sections (OZI-rule violation estimates $R_{\phi/\omega} \sim 10^{-3}$), previous world data is very scarce. CLAS *g11a* dataset – large statistics, fine energy binning and wide kinematic coverage possible.

Charged- and neutral-mode topologies

- ϕ predominantly decays to two kaons. $\phi \rightarrow K^+K^-$ is the "charged-mode" ($bf = 0.491$) while $\phi \rightarrow K_S^0 K_L^0$ is the "neutral-mode" ($bf = 0.34$).
- Charged-mode:
  - Select "+:+" events, kinematically fit to $\gamma p \rightarrow \phi p \rightarrow K^+(K^-)p$ and place 10% confidence level cut.
  - Being a two-track topology, the charged-mode has the largest statistics. 10-MeV $\sqrt{s}$ binning possible.
- Neutral-mode:
  - Select "+:+:-" events, kinematically fit to $\gamma p \rightarrow \phi p \rightarrow K_S^0(K_L^0)p \rightarrow \pi^+\pi^-(K_L^0)p$ and place 10% confidence level cut.
  - Lower statistics, minimum 30-MeV $\sqrt{s}$ binning.

Event-selection: timing cuts

- 2-D calculated mass cut on p, K^+ (charged-mode)

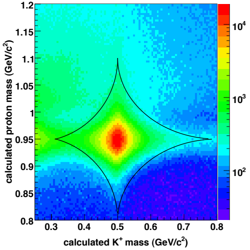

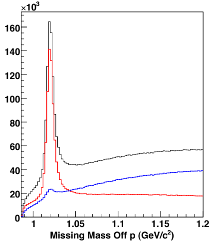

accepted
rejected

- 2-D ΔTOF cut on p, π^+ (neutral-mode)

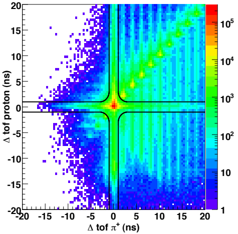

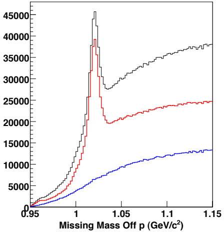

EVENT-SELECTION CONTD.

- K_S^0 selection cut (neutral-mode): 0.49 GeV $\leq M(\pi^+, \pi^-) \leq$ 0.505 GeV.

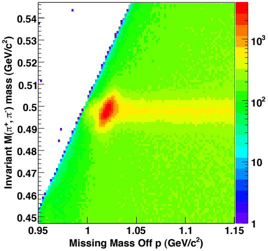

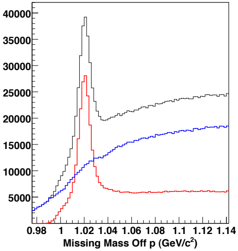

accepted, rejected

Charged-mode topology and ϕ-$\Lambda(1520)$ overlap

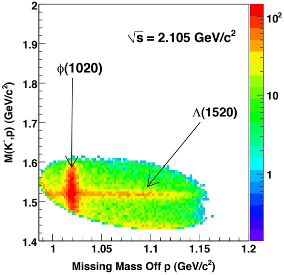

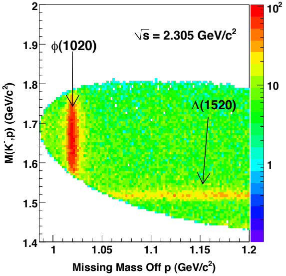

- Consider $\sqrt{s} \rightarrow pK^+K^-$ as a 3-body decay.
- Look at Dalitz-plot of $M(K^+, K^-)$ *vs.* $M(p, K^-)$.
- If $M(K^+, K^-)$ fixed at ϕ mass, $M(p, K^-)$ is bound, limits depending on $\sqrt{s}$.
- Overlap region is only between 2 and 2.2 GeV.
- Only for the charged-mode.

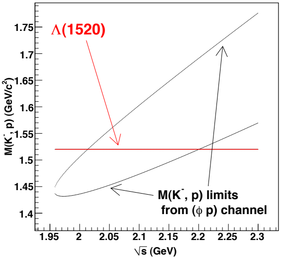

General $M(p, K)$ "Dalitz" cut

- Charged-mode:
  - $\sqrt{s}$ dependent $min(\sqrt{s}) \leq M(p, K^+) \leq max(\sqrt{s})$ always applied.
  - Additional "hard" cut around the $\Lambda(1520)$ mass: $|M(p, K^+) - 1.52| \leq \delta$. Trial values of δ were 5, 10 and 15 MeV.
- Neutral-mode:
  - Similarly, $\sqrt{s}$ dependent cut on $M(p, K^0_S)$ and $M(p, K^0_L)$.

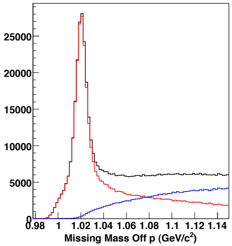

accepted, rejected

Outline

$\phi(1020)$ LINESHAPE

- ϕ width is $\Gamma_0 \approx 4$ MeV, however, its mass being so close to the KK threshold (≈ 0.99 GeV) leads to a unsymmetric lineshape.
- All previous world data used a Gaussian ϕ lineshape for yield extraction fits.
- We've tried to employ a better approximation by taking a mass-dependent width:
$$\Gamma(m) = \Gamma_0 \left(\frac{q}{q_0}\right)^{2L+1} \left(\frac{m_0}{m}\right) \left(\frac{B_0}{B}\right)$$
- $L = 1$ or P-wave $\phi \rightarrow KK$ decay.
- Break-up momentum $q(m) = \sqrt{m^2 - m_K^2}/2$ for a ϕ mass m.
- Barrier-factor $B_{L=1} = \sqrt{2z/(1+z)}$ with $z = q/d$, $d \sim 1$ fm (≈ 0.1973 GeV).
- Subscript 0 denotes evaluation at the ϕ mean mass $m_0 = 1.01946$ GeV.
- Final signal-function in background fits: Voigtian with BW width taken as $\Gamma(m)$.

General set-up

- For every event choose N_c (50, 100, 200, 300 as trial values) "closest-neighbor" events in phase-space.
- Relevant phase-space variables were $\cos\theta^{\phi}_{c.m.}$ and ϕ decay angles ϕ^{K}_{HEL} and $\cos\theta^{K}_{HEL}$.
- Helps in preserving correlations among variables in the data.
- Trial background functions were, a general quartic, $f(x) = a\sqrt{x^2 - 4m_K^2} + b(x^2 - 4m_K^2)$, $x > 2m_K$, and $g(x) = a(x - 2m_K) + b(x - 2m_K)^2$, $x > 2m_K$.
- Fits were quite stable with $N_c = 100$-ish. Final results shown used $N_c = 200$.
- Final output: Q-value or signal probability for each event. Weigh event by corresponding Q-value hereon.
- Method already used in earlier $p\omega$, $p\eta/\eta'$, $K^+\Lambda$ and $K^+\Sigma^0$ analyses.

Application: charged-mode

- $\sqrt{s} = 2.095$ GeV bin. Signal weighted by Q and background weighted by $(1-Q)$:

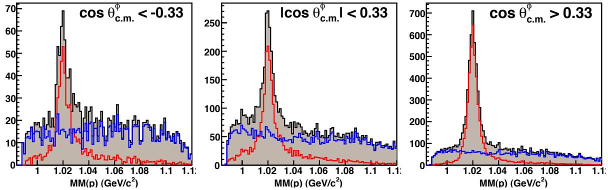

- However, $M(p, K^-) = 1.52$ GeV "band" visible, especially in mid-angles:

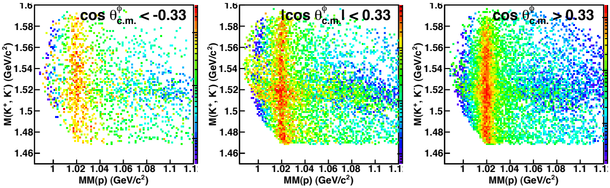

- Apply $|MM(p, K^-) - 1.52 \text{ GeV}| \leq 15$ MeV cut.

Charged-mode: final results

- $\sqrt{s} = 2.095$ GeV
- $\sqrt{s} = 2.405$ GeV
- $\sqrt{s} = 2.705$ GeV

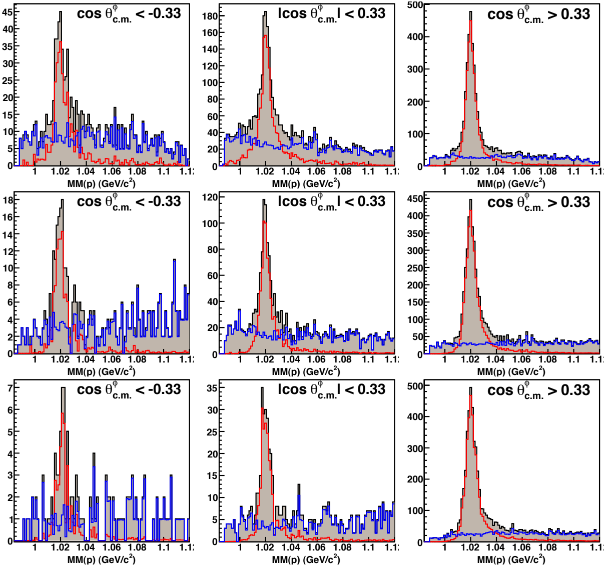

Neutral-mode: results (30-MeV-wide binning)

- $\sqrt{s} = 2.105$ GeV
- $\sqrt{s} = 2.405$ GeV
- $\sqrt{s} = 2.645$ GeV

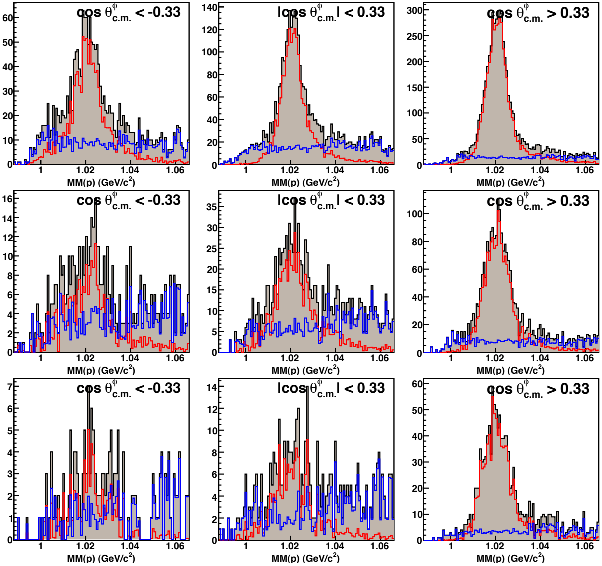

Final Data yields

- Charged-mode occupancy:

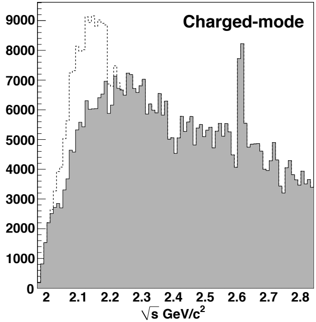

- $\approx$ 0.477 mi – dashed histogram, without 15-mev cut around $\Lambda(1520)$
- $\approx$ 0.436 mi – shaded histogram, with 15-mev cut around $\Lambda(1520)$

- Neutral-mode occupancy:

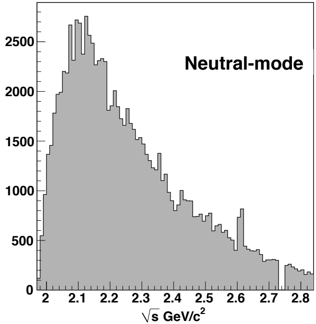

- $\approx$ 0.097 mi
- around one fifth of the charged-mode occupancy

Outline

Acceptance Calculation

- 100 million "Raw" Monte Carlo events for each topology generated flat phase-space and passed thru GSIM to give a set of "Accepted" Monte Carlo events.
- Acc. MC underwent same set of event-selection cuts as actual Data, plus additional efficiency cuts (trigger correction and momentum smearing).
- Fiducial cuts applied to both Data and Acc. MC to remove events belong to regions of the detector that were not well understood (sector-boundaries, extreme forward-going tracks, *et al*)
- Expand the scattering amplitude using a "large" number of s-channel J^P waves:

$$\mathcal{M}(\sqrt{s}, \cos\theta^{\phi}_{c.m.}) \sim \sum_{J^P} \alpha^{J^P}_{MP,LS} \, \mathcal{A}^{\gamma p \to J^P \to \phi p, MP, LS}_{m_\gamma, m_i, m_f, m_\phi}(\sqrt{s}, \cos\theta^{\phi}_{c.m.})$$

- $J^P = \{\frac{1}{2}^{\pm}, \frac{3}{2}^{\pm}, \cdots, \frac{11}{2}^{\pm}\}$ seemed a large enough set to fit the data. $\alpha^{J^P}_{MP,LS}$ are complex numbers (56 real fit parameters)

Fit quality checks

Charged-mode, low $\sqrt{s}$ bin

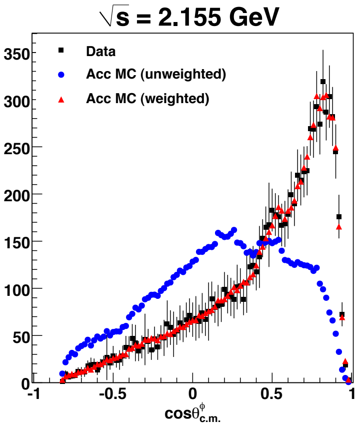

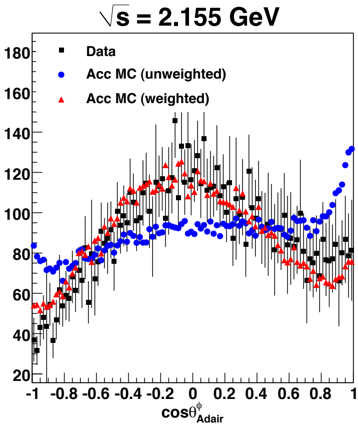

Fit quality checks (contd.)

Charged-mode, high $\sqrt{s}$ bin

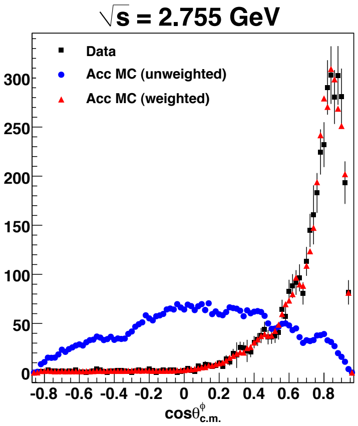

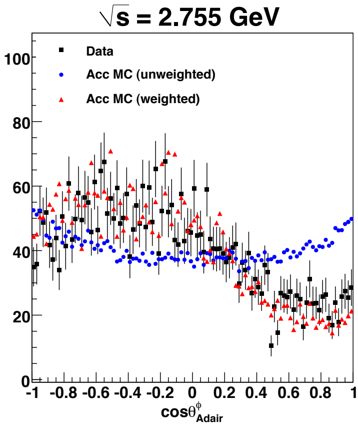

Differential cross sections

Backward-angles

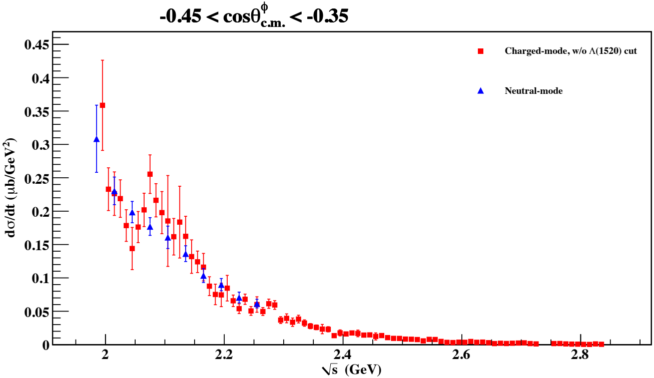

- Neutral-mode (3-track topology) is *highly* statistics limited towards high $\sqrt{s}$ backward-angles.

Differential cross sections (contd.)

Mid-angles

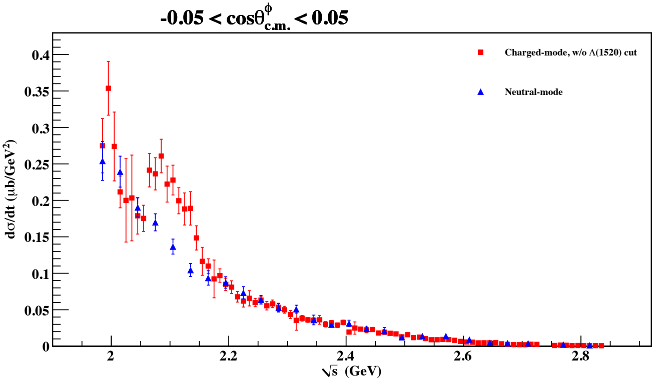

- Clearly, around $\sqrt{s} \approx 2.1$ GeV, the ϕ-$\Lambda(1520)$ overlap is making a difference.

Differential cross sections (contd.)

Forward-angles

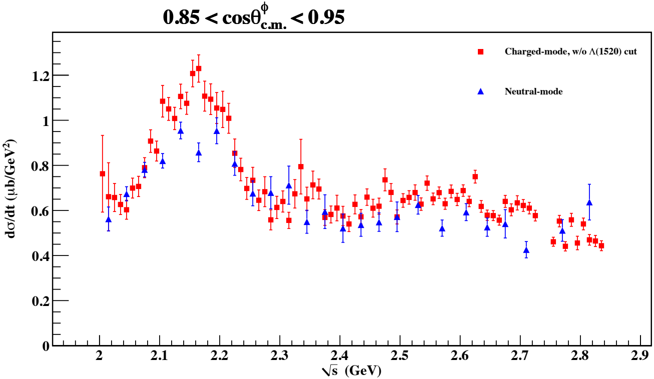

- "Structure" around $\sqrt{s} \approx 2.2$ GeV in both topologies, *probably* independent of the ϕ-$\Lambda(1520)$ overlap issue.
- Above $\sqrt{s} > 2.5$ GeV, $d\sigma/dt$ independent of s at forward angles – diffractive Pomeron exchange.

THE $\sqrt{s} \approx 2.1$ GEV "STRUCTURE"

- Ozaki, Scholten *et al.* (PRC 80, 035201 (2009)): $K\Lambda(1520)$ and ϕp channels couple.

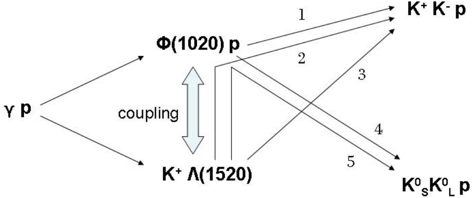

- Coupling either via t-channel on-shell K exchange.
- And/or s-channel high strangeness content resonance exchange.
- Produces $\sqrt{s} \approx 2.1$ GeV "structure" in both cross-sections and spin density matrix elements.

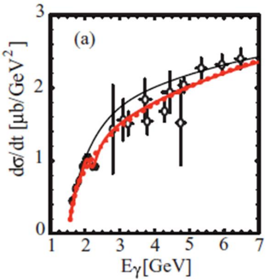

The $\sqrt{s} \approx 2.1$ GeV "structure" (contd.)

- Pomeron slope from fit to $d\sigma/dt = C_{\phi}e^{-B_{\phi}|t-t_0|}$: $B_{\phi} \approx 3$ GeV$^{-}2$.

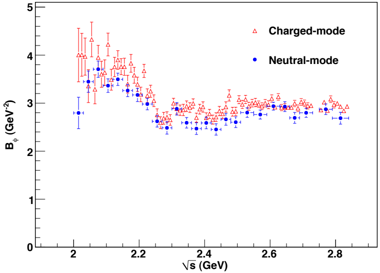

- The "bump" around $\sqrt{s} \sim 2.1$ GeV: most probably, the simple diffractive Pomeron exchange picture no longer valid.

$R_{\phi/\omega}$ AND FLAVOR-INDEPENDENCE

Sibirtsev, *et al* PRD 71, 094011 (2005):

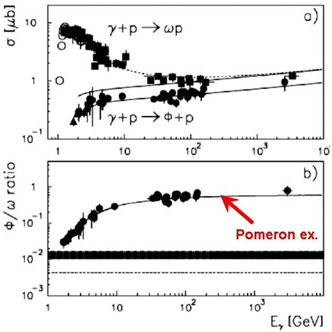

$R_{\phi/\omega}$ as a function of $(\sqrt{s}, \cos\theta^{\phi}_{c.m.})$: ($g11a$ CLAS data)

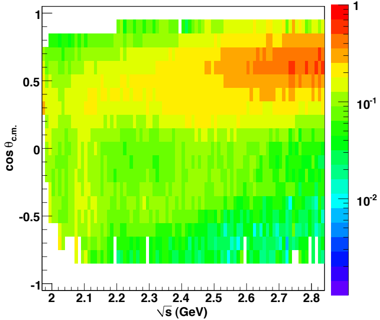

- $R_{\phi/\omega}$ is generally small (OZI-suppression).
- Qualitatively agrees with Donnachie-Landshoff model: quark-quark-Pomeron coupling $\sim \beta_u \beta_s \bar{u}' \gamma_\mu u$. Couplings β almost flavor-independent. In the diffractive limit where Pomeron dominates, $R_\phi/\omega \to 1$

Comparison with previous world data

CLAS $g6$

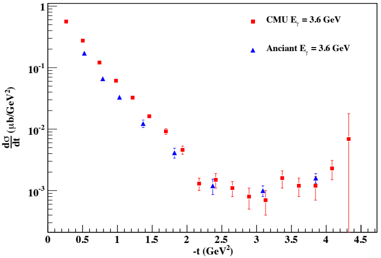

Daresbury

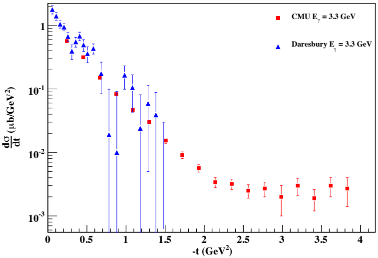

- Main goal of $E_\gamma = 3.6$ GeV CLAS $g6$ (Anciant) data was to look for the backward-angle rise at large $|t|$.
- Slightly lower than CMU $g11a$ around $|t| \sim 1$ GeV, but otherwise good agreement.
- Daresbury data had huge error bars, but fair agreement with our results.

Comparison with SAPHIR (2002)

- SAPHIR, Barth *et al.*, 2002 data (in green).
- CLAS charged-mode in red, and neutral-mode in blue. Energy bin chosen closest to the SAPHIR bin-center.

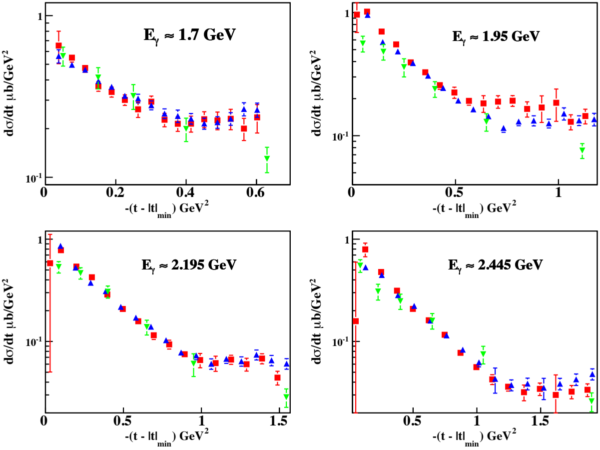

Outline

Spin Density Matrix Elements

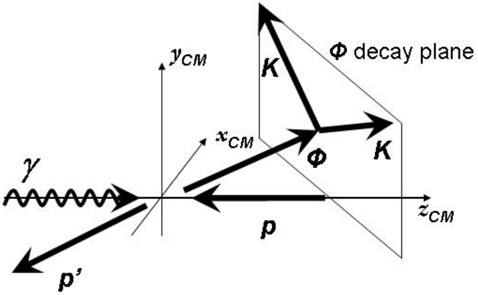

- Choose spin quantitation axis as the beam dirn. $\hat{z}_{CM}$ (Adair frame).
- ϕ rest frame decay angles: θ_{Ad} and φ_{Ad}.
- With unpolarized beam and target, $\rho^0_{MM'}$ only accessible.
- Two *equivalent* methods for extracting SDME.

- PWA method, direct construction of the ϕ density matrix using Mother fit results:

$$\rho^0_{MM'} = \frac{\sum \mathcal{A}^M \mathcal{A}^{M'*}}{\sum |\mathcal{A}^M|^2 + |\mathcal{A}^{M'}|^2},$$

where M, M' are ϕ spin-projections and incoherent sum is over the spins of γ, p, and p'.

- Schilling's method, fit to an intensity distribution:

$$\mathcal{I}(\sqrt{s}, \cos\theta^{\phi}_{c.m.}) \sim \frac{1}{2}(1-\rho^0_{00}) + \frac{1}{2}(3\rho^0_{00}-1)\cos^2_{Ad} - \rho^0_{1-1} sin^2\theta_{Ad}\cos 2\varphi_{Ad}$$
$$-\sqrt{2}Re\rho^0_{10} sin2\theta_{Ad}\cos\varphi_{Ad}$$

Compare PWA and Schilling's method

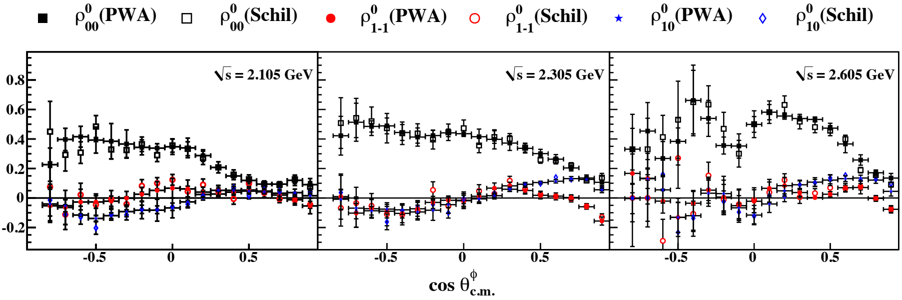

- Very good agreement between the two methods.
- Overall trend of $p\phi$ SDME similar to $p\omega$ case.
- All ρ^0 elements $\rightarrow$ 0 at forward angles, and ρ^0_{1-1} and ρ^0_{10} are small.

SDME, charge-mode topology w/ $\Lambda(1520)$ cut

Backward-angles

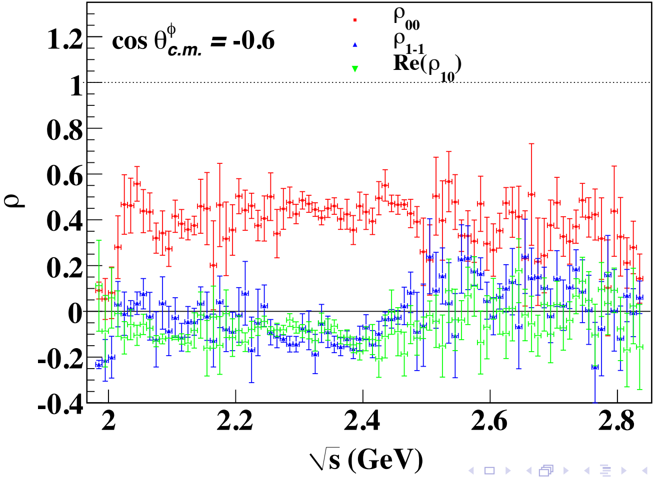

SDME, charge-mode topology w/ $\Lambda(1520)$ cut

Mid-angles

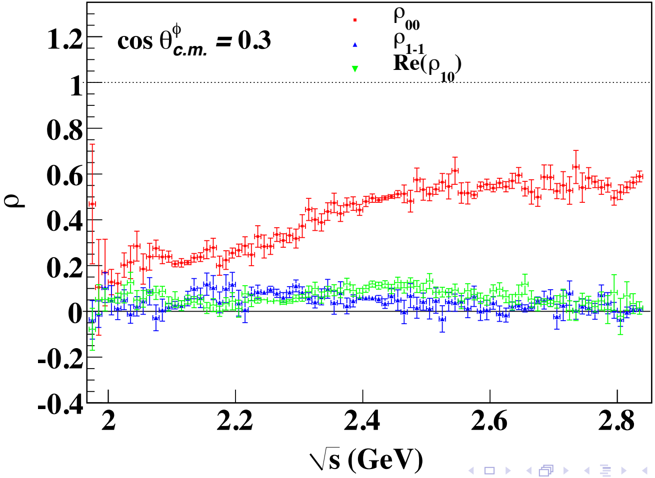

SDME, charge-mode topology w/ Λ(1520) cut

Forward-angles

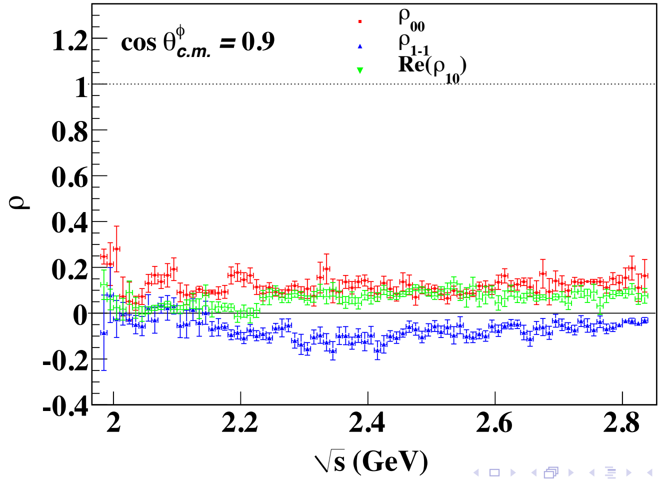

Charged- and neutral-mode comparison for ρ_{00}

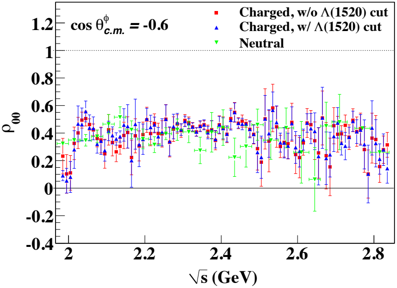

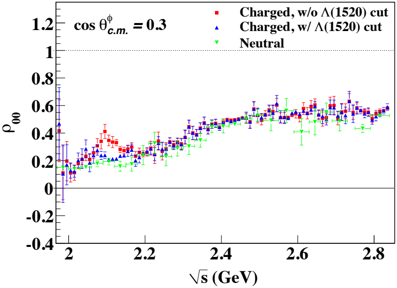

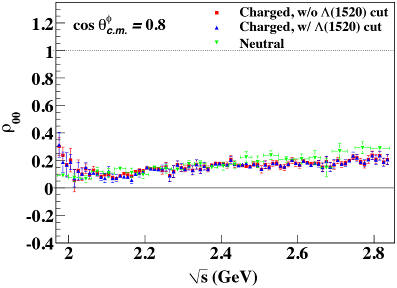

- Generally, very good agreement between the two topologies.
- Only exception is the "bump" at $\sqrt{s} \approx 2.1$ GeV towards the mid- and backward-angles.
- Due to $\Lambda(1520)$?

A Caveat

- Question: does the P-wave KK for the ϕ interfere with the underlying S-wave?

- Fries *et al* (DESY, Nucl. Phys. **B143**, 408, 1978) – $M(KK)$ dependent SDME'S. Claim, S-wave is not just non-resonant, but also resonant (a_0, f_0) contributions.

- Similar ideas echoed in CLAS $g6$ paper, McCormick *et al*, PRC **69** 032203(R) (2004). Integrate Schilling's equation over the azimuthal angle (φ_K) and fit to:

$$dN/d\cos\theta_K \sim (1-\rho_{00})\sin^2\theta_K + 2\rho_{00}\cos^2\theta_K + \alpha\cos\theta_K + \kappa$$

- α is the interference term and κ is the flat S-wave background. Claim: *fits don't work without α and κ*

- Fits might not work because you haven't acceptance corrected properly. Acceptance is *not* flat in φ_K. Plus, Schilling's equation has cross-terms between φ_K and θ_K variables.

- Other reasons: SDME's depend on both W and $\cos\theta_\phi^{c.m.}$. All previous analyses had either huge angular or energy (or both) binnings.

CAVEAT (CONTD.)

- Example: Helicity frame ρ_{00}. Pure P-wave would give a quadratic distribution in $\cos\theta^K_{Hel}$. However without acceptance correction, data is *not* a symmetric parabola:

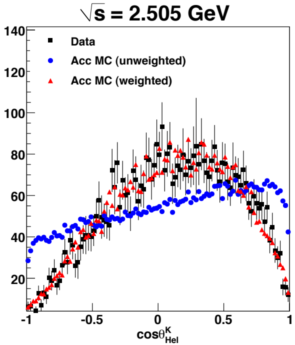

- Distortion caused by acceptance, not *necessarily* by physics.

- Present work and Mike Williams' ω analysis preserved multi-dimensional correlations, accounted for acceptance in the fit and had fine binnings. We didn't require an α.

S- and T-channel Helicity Conservation

- Long-known dilemma: how does the Pomeron couple? 0^+ exchange in t-channel implies TCHC. Experimentally, at high energies TCHC-violation is well-established.
- However, Gilman *et al* (PLB **31**, 387 (1970)) noted, SCHC *roughly* observed for ρ. Gilman's "explanation": SCHC implies TCHC violation.
- Current CLAS results for ω (Williams, PRC **80**, 065208, (2009)), and ϕ (this analysis): TCHC definitely broken. SCHC is also broken.

- $\rho_{00} \sim |\mathcal{A}_{01}|^2 + |\mathcal{A}_{0-1}|^2$
- $\rho_{00} \neq 0$ implies helicity flip
- t-channel: Gottfried-Jackson frame
- s-channel: Helicity frame

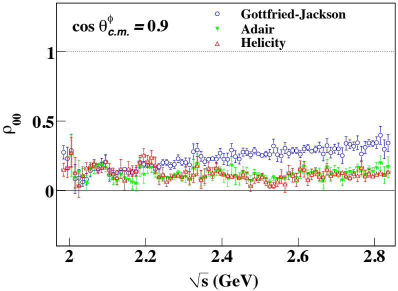

Outline

Summary

- Wide kinematic coverage and high statistics ϕp data for the first time.
- Energy coverage is from near threshold to $\sqrt{s} = 2.84$ GeV and $-0.85 \leq \cos\theta^{\phi}_{c.m.} \leq 0.95$.
- 10-MeV-wide $\sqrt{s}$ binning for charged-mode, and 30-MeV-wide binning for neutral-mode.
- Access to charged-mode (w/ and w/o $\Lambda(1520)$ cut) and neutral-mode results will (hopefully) lead to a better understanding of the $\sqrt{s} \approx 2.2$ GeV "structure".
- Previous ϕ SDME data almost non-existent.
- Full Partial Wave Analysis is underway.

Comparison with Dave Tedeschi's *g11a* results

- Dave Tedeschi (DT) and CMU results comparison: $d\sigma/dt$-**vs**-t.
- DT results show a "dip" at a particular value of t, for each E_γ bin, while CMU shows a more smooth falloff.
- Effect of this "dip" possibly spills over to neighboring t-bins. Except for $t \longrightarrow |t|_{min}$ (extreme forward angles), DT cross-sections are lower.
- DT results generally conform with other ϕ results from the "Phi analysis group" ($g10$, $g6a$), all of which used similar analysis techniques, acceptance calculations, *et al.*

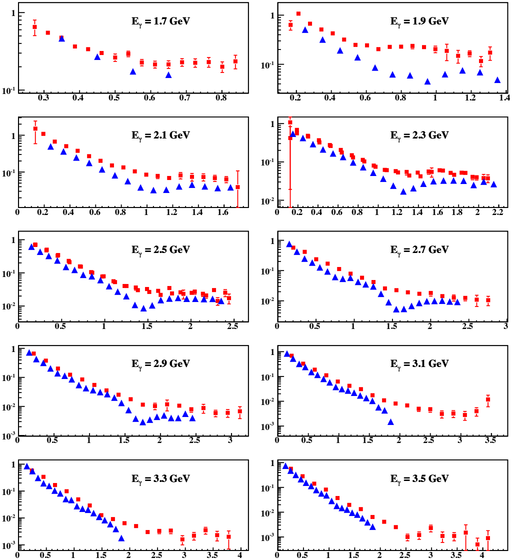

E_γ-VS-t PLOTS AND THE 23^{rd} TOF COUNTER

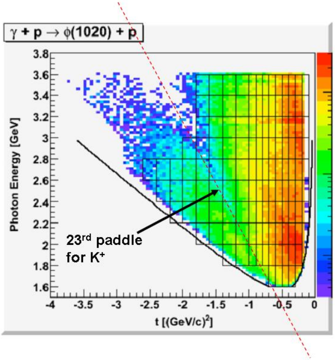

- Position of DT "dip" in E_γ-vs-t tracks K^+ hitting the 23^{rd} TOF paddle.
- 23^{rd} TOF paddle is known to be problematic (removed in some sectors).

23^{rd} TOF counter (contd.)

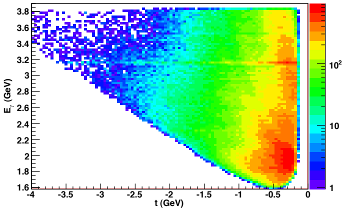

- CMU, same configuration of knocked-out TOF paddles as DT. No such K^+ depletion seen.

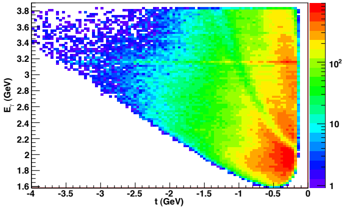

- CMU, 23^{rd} paddle removed in *all* sectors.
- Given (E_γ, t) value corresponds to $\cos\theta_{c.m.}^{proton}$ and proton TOF counter.

Tedeschi acceptance calculation

- MC generated according to $\sim e^{-bt}$ (Pomeron-ish)
- Okay for forward-angles, but for large $|t|$?
- Recall that CMU acceptance calculation was from a direct fit to data.
- Weighted Acc. MC faithfully represented all features in the actual Data.

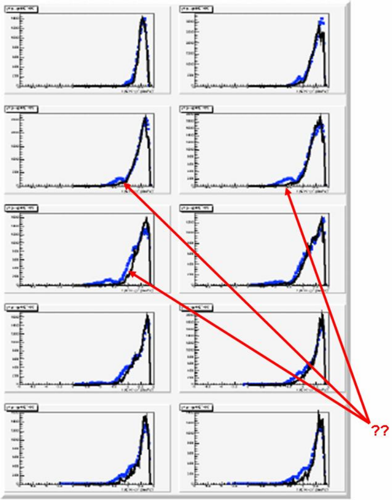

FIG. 8 Comparison of MC (black) with data (blue) for four-momentum transfer in each energy bin.